ELSEVIER

Polymer 42 (2001) 7419–7428

polymer

www.elsevier.nl/locate/polymer

Time and temperature dependence of void closure, healing and interdiffusion during latex film formation

Ertan Arda[a], Önder Pekcan[b,*]

[a]Department of Physics, Trakya University, 22030 Edirne, Turkey
[b]Department of Physics, Faculty of Science and Letters, Istanbul Technical University, Maslak 80626 Istanbul, Turkey

Received 4 September 2000; received in revised form 12 February 2001; accepted 15 February 2001

Abstract

A photon transmission method was used to probe the evolution of transparency during film formation from poly(methyl methacrylate) (PMMA) particles with different molecular weight. The latex films were prepared from low (LM) and high (HM) molecular weighted PMMA particles at room temperature and annealed at elevated temperatures in various time intervals above glass transition (T_g). It was observed that transmitted photon intensities (I_{tr}) from these films increased as the annealing temperature was increased. It is seen from I_{tr} curves that there are two distinct film formation stages, which are named as void closure and interdiffusion processes, respectively. The activation energies for viscous flow and backbone motion were obtained using well-defined models. Viscous flow activation energies (ΔH) were found to be around 150 and 134 kJ/mol for LM and HM films, respectively. Backbone activation energies (ΔE_b) were found to increase from 142 to 199 and 59 to 98 kJ/mol in time of annealing for LM and HM films, respectively. Healing points (τ_H,T_H) were determined and using these time–temperature pairs, healing activation energies (ΔE_H) were measured and found to be 188 and 117 kJ/mol for LM and HM films, respectively.

Keywords: Photon transmission method; Latex film formation; Viscous flow

1. Introduction

Paints, paper coatings, carpet backing [1], textiles, coatings for drug delivery [2], foam mattresses [3] and composites have been well known as applications of latex systems. Film formation from these latexes is a complicated, multistage phenomenon and depends strongly on the characteristics of colloidal particles. In general, aqueous or non-aqueous dispersions of colloidal particles with glass transition temperature (T_g) above the drying temperature are named as hard latex particles. On the other hand, aqueous dispersion of colloidal particles with T_g below the drying temperature is called a soft latex particles. The term 'latex film' normally refers to a film formed from soft particles where the forces accompanying the evaporation of water are sufficient to compress and deform the particles into a transparent, void-free film [4,5]. However, hard latex particles remain essentially discrete and undeformed during the drying process. Film formation from these dispersions can occur in several stages. In both cases, the first stage corresponds to the wet initial state. Evaporation of solvent leads to second stage in which the particles form a close packed array. If the particles are soft, they are deformed to polyhedrons. Hard latex, however, stay undeformed at this stage. Annealing of soft particles causes diffusion across particle–particle boundaries which leads the film to a homogeneous continuous material. Annealing of hard latex system, deformation of particles first leads to void closure [6,7] and then, after the voids disappear, diffusion across particle–particle boundaries starts, i.e. the mechanical properties of hard latex films can be evolved by annealing; after all solvent has evaporated and all voids have disappeared.

After the void closure process is completed, the mechanism of film formation, by annealing of hard latex films is known as interdiffusion of polymer chains followed by healing at polymer–polymer interface. In general, when two identical polymeric materials are brought into contact at a temperature above their glass transition temperature, the junction surface gradually disappears and becomes indistinguishable from any other surface that might be located within the bulk material. Brownian motion drives the polymer chains across the junction until eventually all traces of the original interface are lost; at this point one may say that

* Corresponding author. Tel.: +90-212-285-3340; fax: +90-212-285-6386.
E-mail address: pekcan@itu.edu.tr (Ö. Pekcan).

0032-3861/01/$ - see front matter
PII: S0032-3861(01)00131-8

junction has 'healed'. Many years ago Voyutskii [8] suggested that the formation of a continuous, strong and water-impermeable film involves polymer diffusion across the junction of identical polymer particles. The molecular interpenetration of the healing process is related to the phenomenon of self-diffusion in bulk polymers, but the two are not identical. In self-diffusion, polymer coils move over distances many times their mean diameter, whereas healing is essentially complete in the time it takes a polymer coil initially next to the junction surface to move halfway across it. The 'healing time' (τ_H) can then be comparable to the conformational relaxation time (τ_e) of a polymer chain. When polymer chains are much longer than a certain length diffusion of chains is pictured as a worm-like motion described by the reptation model, proposed by de Gennes [9]. The reptation time (T_r) gives the time necessary for a polymer to diffuse a sufficient distance for all memory of the initial tube to be lost. Prager and Tirrell [10] derived a relation for the crossing density of the chains by using the reptation model during the healing process. Wool and O'Connor [11] employed reptation to study crack healing in terms of several stages, including wetting, diffusion and randomization, where at the end of the wetting stage, potential barriers associated with the inhomogeneities at the interface disappear and chains are free to move across the interface by a randomization process.

Transmission electron microscopy (TEM) has been used to examine the morphology of dried latex films [12,13]. These studies have shown that in some instances the particle boundaries disappeared over time, but in other cases the boundaries persisted for months. It was suggested that in the former case particle boundaries healed by polymer diffusion across the junction. In the last few years, it has become possible to study latex film formation at the molecular level. Small-angle neutron scattering (SANS) was used to examine deuterated particles in a protonated matrix. It was observed that the radius of the deuterated particle increased in time as the film was annealed [14] and as the polymer molecules diffused out of the space to which they were originally confined. The process of interparticle polymer diffusion has also been studied by the direct energy transfer (DET) method, using transient fluorescence measurements [15,16] in conjunction with latex particles labelled with donor and acceptor chromophores. Steady state fluorescence (SSF) method combined with DET was also used for studying film formation from hard latex particles [17–20]. Extensive review of the subject is given in Ref. [21]. Recently we have performed various experiments with photon transmission method using UV–Vis (UVV) spectrophotometer to study latex film formation from poly(methyl methacrylate) (PMMA) and PS latexes where void closure and interdiffusion processes at the junction surfaces are studied [22–28]. These studies all indicate that the annealing leads to polymer diffusion and mixing as the particle junction heals during latex film formation.

In this work, transparencies of the films formed from low molecular weighted (LM) and high molecular weighted (HM) latexes were studied by measuring the transmitted photon intensities (I_{tr}) by using an UVV spectrophotometer. Various stages of film formation were generated by annealing the dried PMMA latex powders at equal time intervals above the glass transition temperature, T_g of PMMA. Variation in I_{tr} with respect to annealing temperature were used to study the void closure and interdiffusion processes. Healing points (τ_H,T_H) were determined and used to measure the healing activation energies (ΔE_H) which are found to be 188 and 117 kJ/mol for the LM and HM systems, respectively. Void closure equation was derived at the early stage of film formation and used to obtain the activation energy of viscous flow (ΔH) which are measured to be 150 and 134 kJ/mol for LM and HM films, respectively. The model developed by Prager and Tirrell (PT) was employed to measure the backbone activation energies (ΔE_b) for the interdiffusing polymer chains of LM and HM systems which are found to be depending on annealing times.

2. Experimental

Two different batches of PMMA particles were prepared separately in a two-step process. First methyl methacrylate (MMA) was polymerized to low conversion in cyclohexane in the presence of poly(isobutylene) (PIB) containing 2% isoprene units to promote grafting. The graft copolymer so produced served as a dispersant in the second stage of polymerization, in which MMA was polymerized in a cyclohexane solution of the polymer. Details have been published elsewhere [29]. In both batches, a stable dispersion of spherical polymer particles were produced with radius ranging from 1 to 3 μm. A combination of ^{1}H-NMR and UV analysis indicated that these particles contain 6 mol% PIB and DSC results show that glass transition temperature, T_g of these particles (HM and LM) are both found to be around 390 K. The particle size of LM and HM particles are measured using scanning electron micrographs of these particles and found to be 2 and 0.5 μm, respectively (These particles were prepared by Williamson in Winnik's Laboratory in Toronto). In the first and second batch of particles, molecular weights of graft PMMA were measured as $M_w = 2.15 \times 10^5$ and $M_w = 1.10 \times 10^5$, respectively. These particles are used to prepare HM and LM samples, respectively. The polydispersities of the corresponding PMMA were 1.49 and 2.33 for the HM and LM particles. Two different sets of films were prepared from the dispersions of HM and LM particles in heptane by placing same number of drops on a glass plates with the size of 0.9×3.2 cm^2. Each set of samples contains seven different films. Annealing process of the latex films were performed in an oven in air above T_g of PMMA after evaporation of heptane, in 60, 30, 15, 10, 5, 2.5 and 1 min time intervals at elevated temperatures between 383–483 and 383–543 K for LM and HM film samples, respectively. The temperature

was maintained within ±1 274 K during annealing. Samples were weighed before and after film casting to determine the latex contents and film thicknesses. The particle sizes were used for the calculation of the thickness of the films. UVV experiments were carried out with the model Lambda 2S UVV spectrometer from Perkin–Elmer and transmittance of the films was detected between 300 and 400 nm. All measurements were carried out at room temperature after the annealing processes were completed. Errors in UVV measurements originate mostly from the surface inhomogeneities (voids and cracks) of film samples, which cause variation in I_{tr} intensities. Signal to noise ratio in I_{tr} is quite low (1–2%) and can be neglected in error estimations.

3. Results and discussions

Transmitted photon intensities, I_{tr} from the LM and HM latex films are plotted versus annealing temperature for various time intervals are shown in Fig. 1a and b, respectively. Data in Fig. 1a and b all indicate that films become transparent when they are annealed. In other words films scattered less light due to homogenization during film formation. When the I_{tr} intensities are compared for the LM and HM film samples, it is seen that the HM film needs higher annealing temperatures to reach the same transparency as that of the LM film for the same time intervals. Fig. 2 compares the I_{tr} curves for the LM and HM samples for the 60 min annealing time interval. Relatively small I_{tr} intensities are observed in latex films annealed at short time intervals, indicating that some photons dissipate i.e. cannot reach the photodiode after they pass through these films. It was observed that increasing the annealing time from 15, 30 and 60 min, for increasing annealing temperature that I_{tr} becomes larger. These changes in I_{tr} may be interpreted that annealing the films for larger times result in the formation of more transparent films. The increase in I_{tr} may be interpreted by the mechanisms of void closure, healing and interdiffusion processes, respectively. Spherical particles that have increasing surface energy flows to intervoids (void closure) at the early stage of annealing where the radius of interparticle voids becomes smaller and film surface becomes more homogeneous, consequently transparency of film starts to increase. If the annealing is carried on, chain segments (minor chains) move across the particle–particle interfaces and therefore latex film becomes more transparent. This process is called healing. At high annealing temperatures the chains gain sufficient kinetic energy to transform its centre of mass across the junction surface (interdiffusion) and therefore latex film becomes fully transparent. In order to have the better feeling for the possible mechanisms, the transmitted photon intensities, I_{tr} from the LM and HM films are plotted versus annealing temperature for 1, 5 and 60 min time intervals in Fig. 3a and b, respectively. It is seen that all I_{tr} intensity curves start to increase at different temperatures

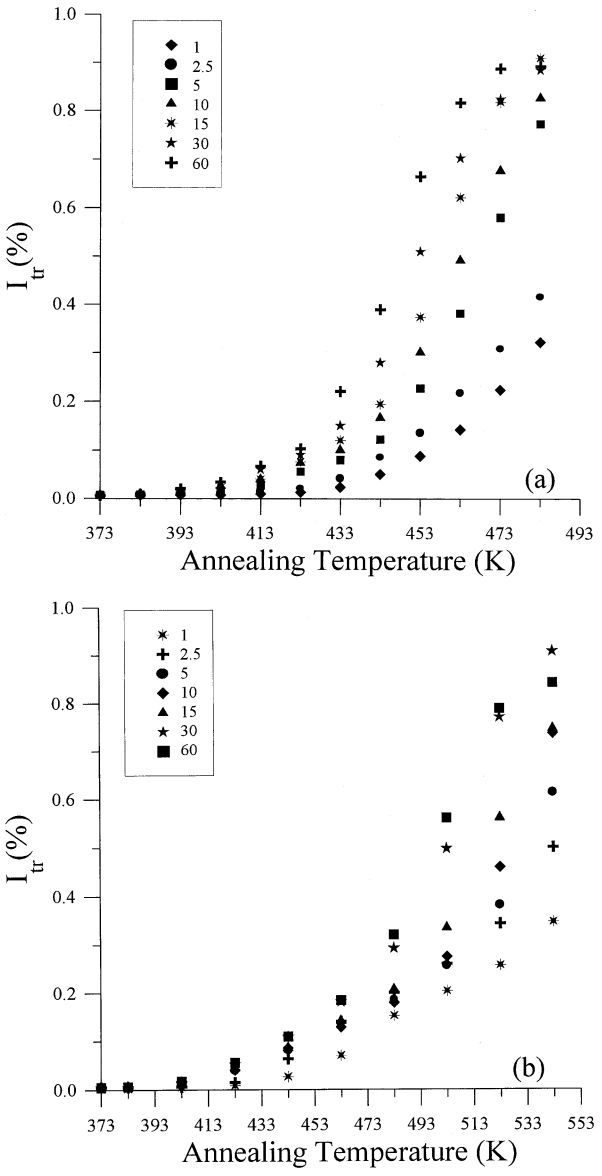

Fig. 1. Plot of I_{tr} versus annealing temperature for 1, 2.5, 5, 10, 15, 30 and 60 min time intervals as indicated in the rectangle, for the latex films: (a) LM, (b) HM.

depending on their annealing times. All the plots in Fig. 3a and b presents two distinct linear regions. These regions can be explained by the void closure and interdiffusion mechanisms during film formation process. Intersections between the two broken lines in Fig. 3a and b present the healing (τ_H,T_H) points.

3.1. Viscous flow and void closure mechanism

In order to quantify the behaviour of I_{tr} at the early stage of annealing, a phenomenological void closure model is introduced. Particle deformation and void closure between particles can be induced by shearing stress which is generated by surface tension of polymer i.e. polymer air interfacial tension. The void closure kinetics can determine the

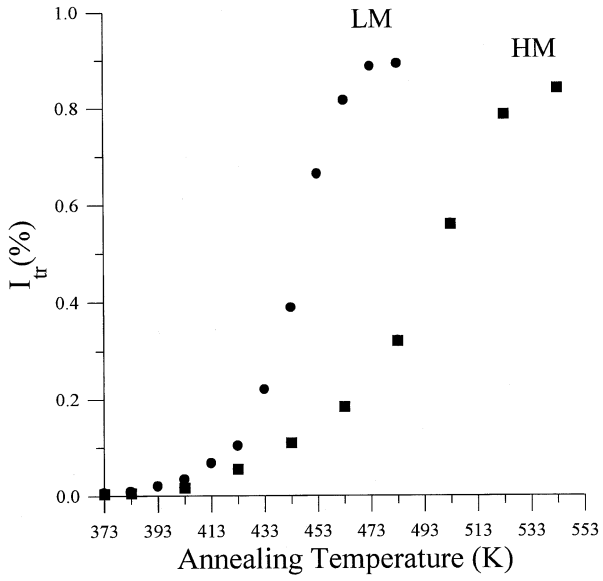

Fig. 2. Comparison the I_{tr} values of LM and HM samples anneal for 60 min time intervals.

time for optical clarity and film formation. An expression to relate the shrinkage of spherical void of radius, r, to the viscosity of surrounding medium, η, was derived and given by the following relation [30]

$$\frac{dr}{dt} = -\frac{\gamma}{2\eta}\left(\frac{1}{\rho(r)}\right), \tag{1}$$

where γ is the surface energy, t is time and $\rho(r)$ is the relative density. It has to be noted that here surface energy causes a decrease in void size and the term $\rho(r)$ varies with the microstructural characteristics of the material, such as the number of voids, the initial particle size and packing. Here $\rho(r)$ can be defined as a volume ratio of polymeric material to voids where as r goes to zero $\rho(r)$ increases, however for large r values $\rho(r)$ decreases. Eq. (1) is quite similar to one which was used to explain the time dependence of the minimum film formation temperature during latex film formation [7,31]. If the viscosity is constant in time, integration of Eq. (1) gives the relation as

$$t = -\frac{2\eta}{\gamma}\int_{r_0}^{r}\rho(r)\,dr, \tag{2}$$

where r_0 is the initial void radius at time $t = 0$.

The dependence of the viscosity of polymer melt on temperature is affected by the overcoming of the forces of macromolecular interaction which enables the segments of polymer chain to jump over from one equilibration position to another. This process happens at temperatures at which free volume becomes large enough and is connected with the overcoming of the potential barrier. The height of this barrier can be characterized by free energy of activation, ΔG during viscous flow. Frenkel–Eyring [32] theory produces the following relation for the temperature dependence of

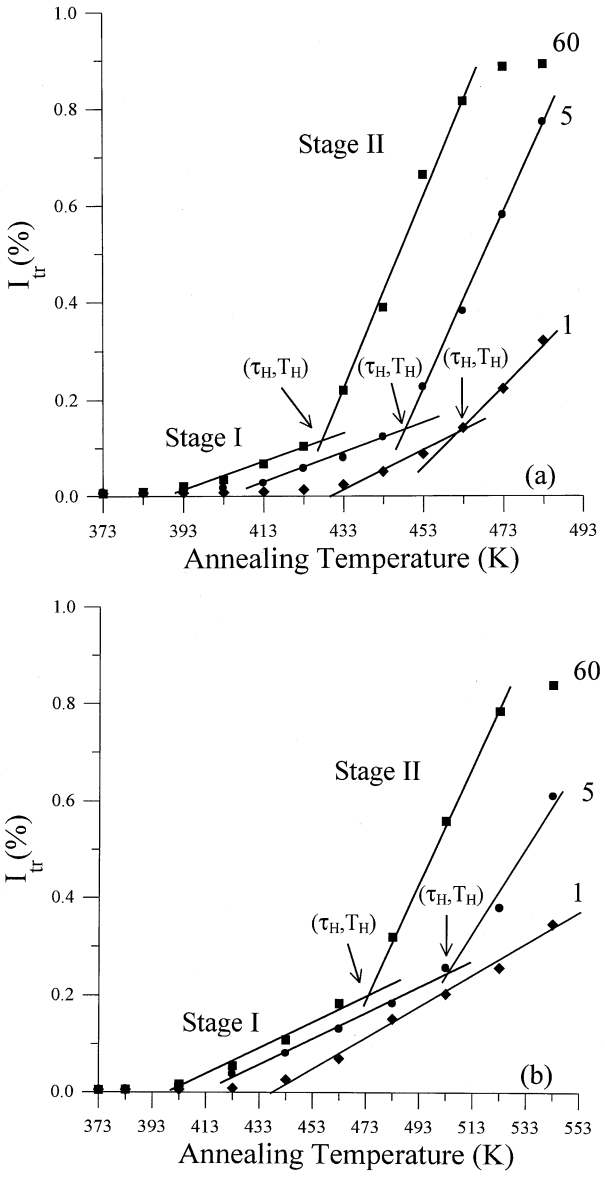

Fig. 3. Plot of I_{tr} versus annealing temperature for 1, 5 and 60 min time intervals for a-LM, b-HM latex films. Stages I and II present the void closure and interdiffusion processes.

viscosity

$$\eta = \frac{N_0 h}{V}\exp(\Delta G/kT), \tag{3}$$

where N_0 is the Avagadro's number, h is Planck's constant, V is molar volume and k is the Boltzmann constant. It is known that $\Delta G = \Delta H - T\Delta S$, then Eq. (3) can be written as

$$\eta = A\exp(\Delta H/kT), \tag{4}$$

where ΔH is the activation energy of viscous flow i.e. the amount of heat which must be given to one mole of material for creating the act of a jump during viscous flow. ΔS is the entropy of activation of viscous flow. Here A present a constant for the related parameters. Combining Eqs. (2)

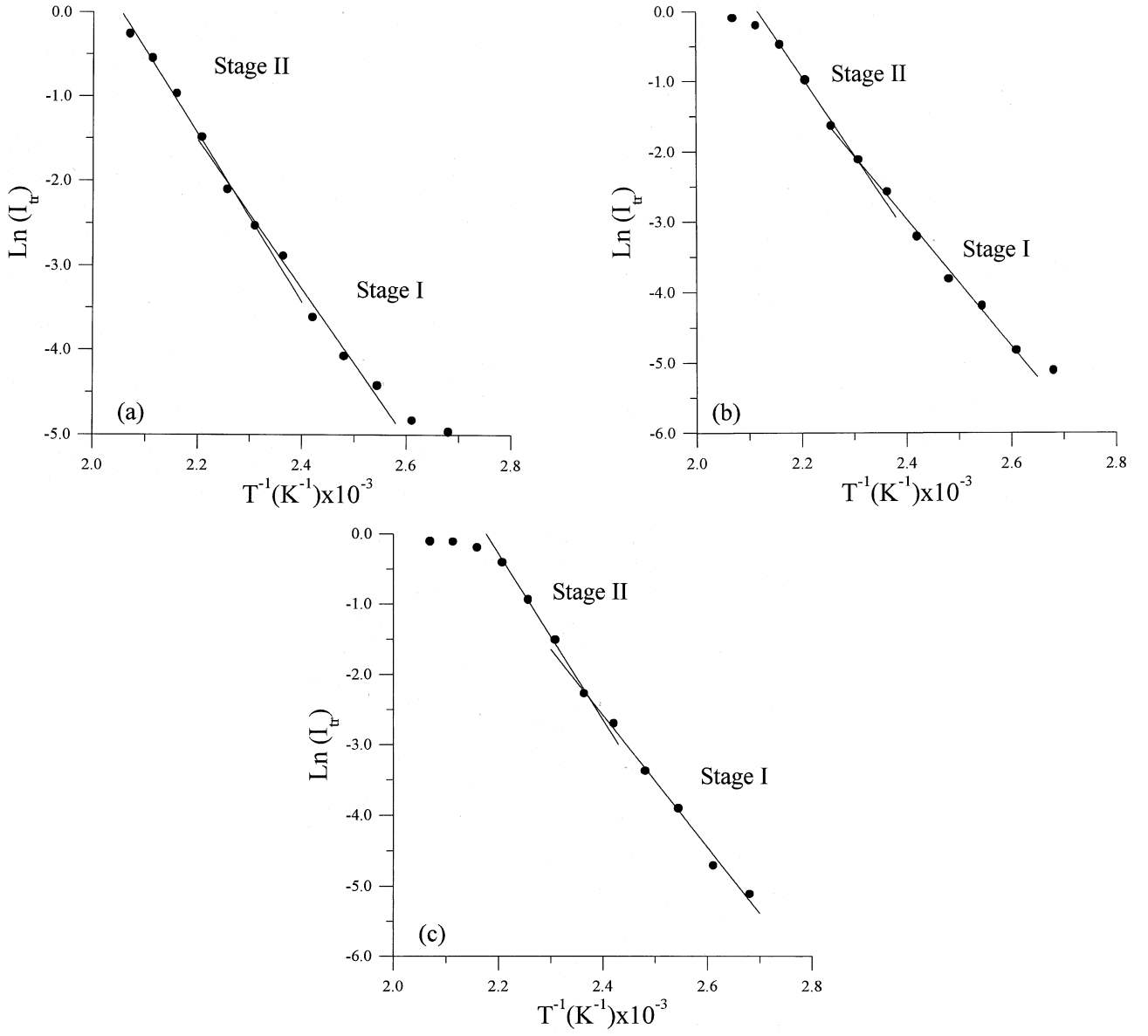

Fig. 4. Logarithmic plots of the data presented in Fig. 1a versus reverse of annealing temperature (T^{-1}) for (a) 5, (b) 15 and (c) 60 min time intervals. Stages I and II present the void closure and interdiffusion processes.

and (4) the following useful equation is obtained

$$t = -\frac{2A}{\gamma}\exp\left(\frac{\Delta H}{kT}\right)\int_{r_0}^{r}\rho(r)\,\mathrm{d}r. \tag{5}$$

Eq. (5) can be employed by assuming that the interparticle voids are in equal size and number of voids stay constant during film formation (i.e. $\rho(r) \propto r^{-3}$), then integration of Eq. (5) gives the relation

$$t = \frac{2AC}{\gamma}\exp\left(\frac{\Delta H}{kT}\right)\left(\frac{1}{r^2} - \frac{1}{r_0^2}\right), \tag{6}$$

where, C is a constant related to relative density $\rho(r)$. It is well established that decrease in void size causes an increase in mean free path of a photon which then results an increase in I_{tr} intensity [27]. Then the assumption can be made that I_{tr} is inversely proportional to the void radius, r and Eq. (6) can be written as

$$t = \frac{2AC}{\gamma}\exp\left(\frac{\Delta H}{kT}\right)I_{tr}^2. \tag{7}$$

Here r_0^{-2} is omitted from the relation since it is very small compared to r^{-2} values after void closure processes start. Eq. (7) can be solved for I_{tr} to interpret the results in Fig. 1a and b as

$$I_{tr}(T) = S(t)\exp\left(-\frac{\Delta H}{2kT}\right), \tag{8}$$

where $S(t) = (\gamma t/2AC)^{1/2}$. For a given time the logarithmic

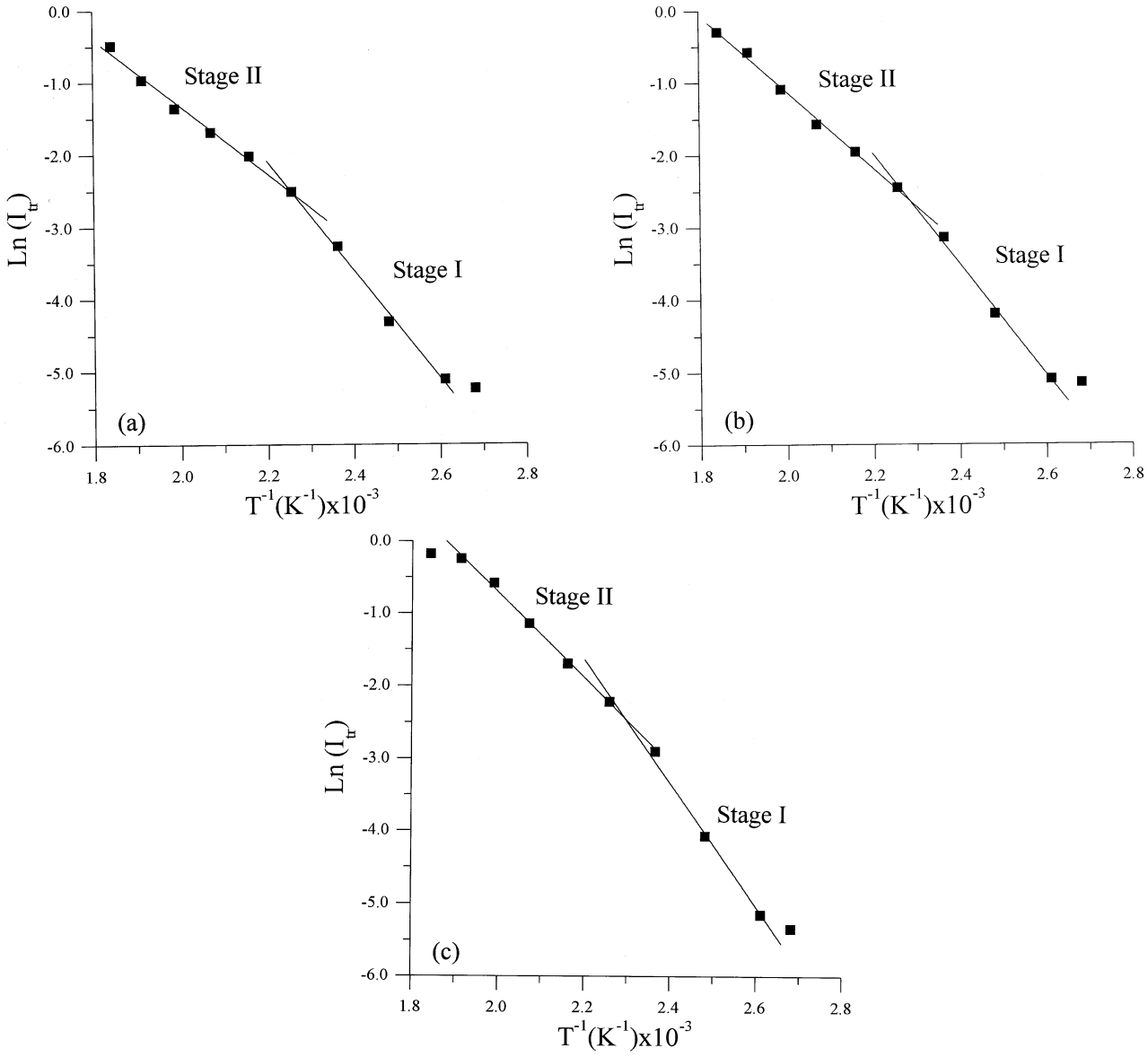

Fig. 5. Logarithmic plots of the data presented in Fig. 1b versus reverse of annealing temperature (T^{-1}) for (a) 5, (b) 15 and (c) 60 min time intervals. Stage I and stage II present the void closure and interdiffusion processes.

form of Eq. (8) can be written as follows

$$\ln I_{tr}(T) = \ln S(t) - \frac{\Delta H}{2kT}. \quad (9)$$

$\ln I_{tr}$ versus T^{-1} plots of the data in Fig. 1a and b are presented in Figs. 4 and 5, respectively, for a-5, b-15 and c-60 min time intervals. All the plots in Figs. 4 and 5 present two distinct regions, where Stages I and II presents void closure and interdiffusion processes, respectively. Stage I in Figs. 4 and 5 are fitted to Eq. (9) and ΔH values are obtained from the slopes of figures. ΔH values are plotted versus annealing time intervals in Fig. 6a and b for LM and HM films, respectively. The averaged ΔH values were found to be 150 and 134 kJ/mol for LM and HM films, respectively. The activation energy of viscous flow i.e. the dependence of viscosity on temperature is determined by the structure of polymer chain. In other words the type of branches and the presence of polar groups in the chain determine the kinetic flexibility of polymer. For carbon chain polymers ΔH are found to be 21–29 kJ/mol (polyethylene). ΔH reaches to the value of 63 kJ/mol for PIB. For polystyrene whose side groups are phenyl rings ΔH rises to 117 kJ/mol. ΔH is much higher for poly(vinyl chloride) (147 kJ/mol) and poly(vinyl acetate) (251 kJ/mol) polymers. Here the ΔH values are found to be very close to poly(vinyl chloride) chains.

3.2. Healing at polymer–polymer interface

It is seen in Fig. 3a and b that, T_H for the onset of increase

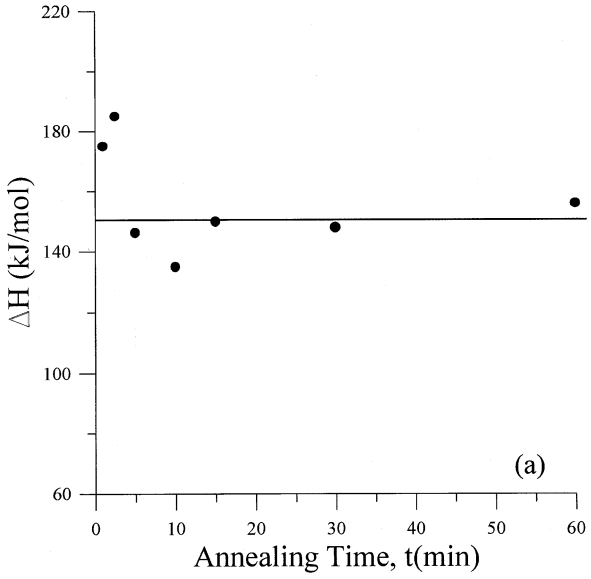

Fig. 6. Plot of viscous flow activation energies (ΔH) versus annealing time (t) for (a) LM, (b) HM films. ΔH values are obtained by fitting the stage I data in Figs. 4 and 5 to Eq. (9).

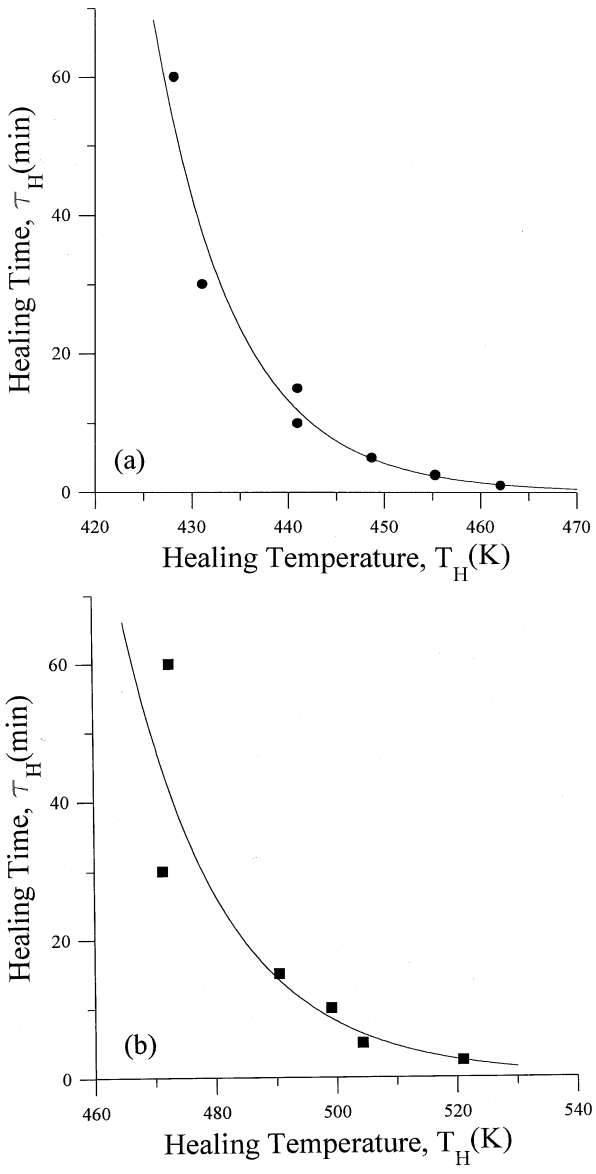

Fig. 7. Plot of the healing points (τ_H,T_H) which obtained from the intersection of broken lines in Fig. 3a and b, for (a) LM, (b) HM film samples.

in I_{tr} values shifted to higher temperatures for smaller annealing time intervals for both LM and HM samples, respectively. This behaviour indicates that for short annealing times films need higher temperature for healing process to be occurred, otherwise it is reversed. (τ_H,T_H) pairs are plotted in Fig. 7a and b for LM and HM film samples, respectively, where it is seen that as τ_H is decreased T_H has to increase to execute the healing process using minor chains, during film formation. Initially, below T_H, due to the sharp particle boundaries or voids between particles, light scatters from the film surface. Increasing of temperature causes wetting which initiates segmental motion and as a result polymer chain segments move across the interface. Subsequently, more light can enter the latex film and the transmission intensity increases.

In order to quantify the results in Fig. 7 we employed the minor chain model developed by Wool et al. [33,34]. They used the reptation model of chain dynamics [9] where by a wriggling motion, a chain on average moves coherently back and forth along the centre line of the tube. The portions of a chain that are no longer in the initial tube increase with time and are referred to as a minor chain of length $l(t)$ see Fig. 8. The conformations of the minor chains are always Gaussian. Kim and Wool [33] derived the average of the $l(t)$ values for times shorter than the tube renewal time (T_r) and found that

$$\langle l^2 \rangle = 2D\tau_H. \quad (10)$$

Here, the curvilinear diffusion coefficient, D, can be in the

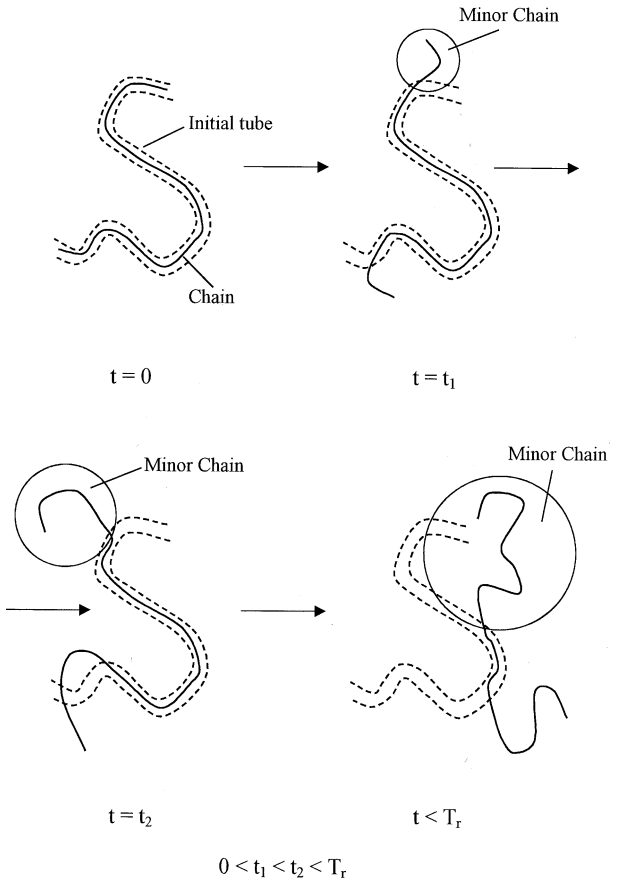

Fig. 8. Disengagement of a Gaussian chain from its initial tube in the reptation model, i.e. the growth of minor chain. T_r is the tube renewal time.

following form at T_H

$$D = D_0 \exp(-\Delta E_H/kT_H), \quad (11)$$

where ΔE_H is the healing activation energy, which is the minimum energy required for a minor chain to move across to the junction surface and k is the Boltzmann constant. If one assumes that $\langle l^2 \rangle$ values are identical at the healing temperatures of each separate set of experiments, then a very useful relation can be obtained from Eqs. (10) and (11)

$$\tau_H = B \exp(\Delta E_H/kT_H), \quad (12)$$

where $B = 2D_0/\langle l^2 \rangle$ is a constant for all sets of experiments in Fig. 7a and b. The fit of Eq. (12) to the data in Fig. 7a and b is shown in Fig. 9a and b, respectively, where the slope of the straight line produced the ΔE_H value as 188 and 117 kJ/mol for LM and HM films, respectively.

3.3. Chain reptation and interdiffusion

When film samples were annealed at elevated temperatures for various time intervals above the (τ_H,T_H), a continuous increase in I_{tr} intensities was observed until they become saturated (see Fig. 3). This further increase in I_{tr} (stage II) can be explained by the increase in transparency of latex film due to the disappearance of particle–particle

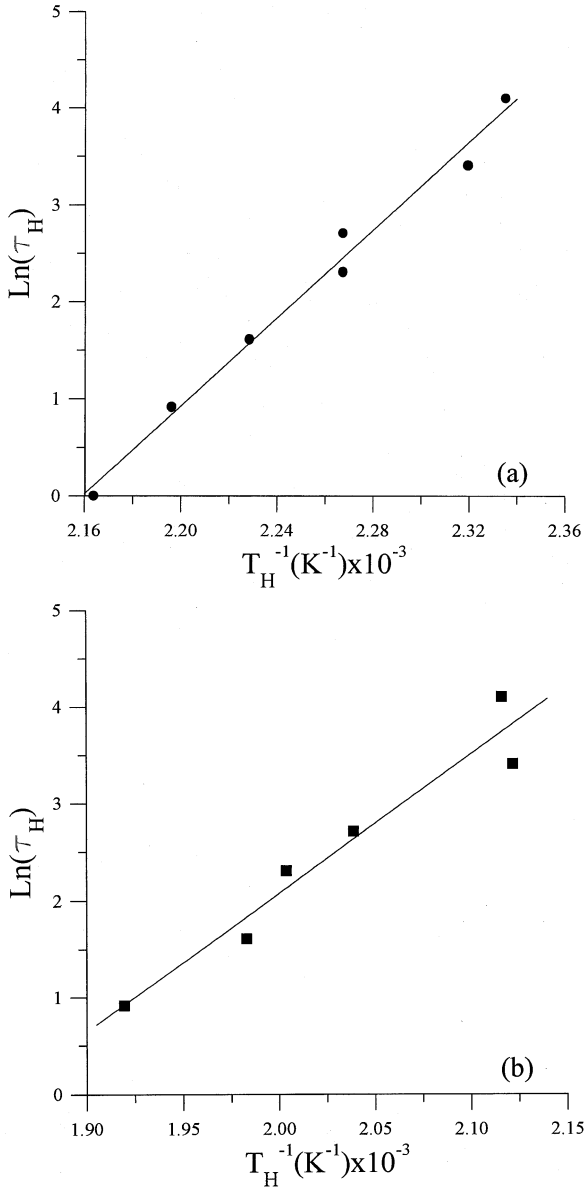

Fig. 9. Arrhenius plot of Eq. (12). Slope of the curve produce ΔE_H value for (a) LM, (b) HM film samples.

boundaries known as interdiffusion. As the annealing temperature is increased, some of the polymer chains cross the junction surface and particle boundaries disappear, and as a result, the transmitted photon intensity I_{tr} increases. The increase in annealing temperature causes total transfer of polymer chains across the boundary, which results completely transparent film.

In order to quantify these results, the PT model [10] for the chain crossing density can be employed. These authors used de Gennes's 'reptation' model [9] to explain configurational relaxation at the polymer–polymer junction where each polymer chain is considered to be confined to a tube in which it executes a random back and forth motion. A homopolymer chain with N freely jointed segments of length L was considered by PT, which moves back and forth by one

segment with a frequency ν. In time the chain displaces down the tube by a number of segments, m. Here, $\nu/2$ is called the 'diffusion coefficient' of m in one dimensional motion. PT calculated the probability of the net displacement with m during time t in the range of $n-\Delta$ to $n-(\Delta+\mathrm{d}\Delta)$ segments. A Gaussian probability density was obtained for small times and large N. The total 'crossing density' $\sigma(t)$ (chains per unit area) at junction surface then was calculated from the contributions due to chains still retaining some portion of their initial tubes, $\sigma_1(t)$ plus a remainder, $\sigma_2(t)$. Here the $\sigma_2(t)$ contribution (backbone motion) comes from chains which have relaxed at least once. In terms of reduced time $\tau = 2\nu t/N^2$ the total crossing density can be written as

$$\sigma(\tau)/\sigma(\infty) = 2\pi^{-1/2}\left[\tau^{1/2} + 2\sum_{k=0}^{\infty}(-1)^n[\tau^{1/2}\exp(-k^2/\tau) - \pi^{-1/2}erfc(k/\tau^{1/2})]\right]. \quad (13)$$

For small τ values the summation term in the above equation is very small and can be neglected, which then results in

$$\sigma(\tau)/\sigma(\infty) = 2\pi^{-1/2}\tau^{1/2}. \quad (14)$$

This was predicted by de Gennes on the basis of scaling arguments. In order to compare our results with the crossing density of the PT model, the temperature dependence of $\sigma(\tau)/\sigma(\infty)$ can be modelled by taking into account the following Arrhenius relation for the linear diffusion coefficient

$$\nu = \nu_0 \exp(-\Delta E_b/kT). \quad (15)$$

Here ΔE_b is defined as the activation energy for the backbone of polymer chain. Combining Eqs. (14) and (15) a useful relation is obtained as

$$\frac{\sigma(T)}{\sigma(\infty)} = R\exp(-\Delta E_b/2kT), \quad (16)$$

where $R = (8\nu_0 t/\pi N^2)^{1/2}$ is a temperature independent coefficient.

In order to explain the behaviour of I_{tr} at Stage II in Fig. 3a and b it is assumed that I_{tr} is proportional to the crossing density $\sigma(T)$ at the interface, then the phenomenological equation can be written as

$$\frac{I_{tr}(T)}{I_{tr}(\infty)} = R\exp(-\Delta E_b/2kT). \quad (17)$$

The activation energies (ΔE_b) of backbone motion were produced by fitting the stage II data in Figs. 4 and 5 to logarithmic form of Eq. (17). The observed ΔE_b values are plotted against annealing time in Fig. 10a and b for LM and HM films, respectively, where it is seen that smaller ΔE_b values correspond to the short annealing time intervals for both of LM and HM films. This behaviour can be explained with the following sentence. Short chains cross the interface at short annealing times, which need smaller energy to execute backbone motion. However long chains need longer annealing time intervals to cross the interface, which poses large activation energies.

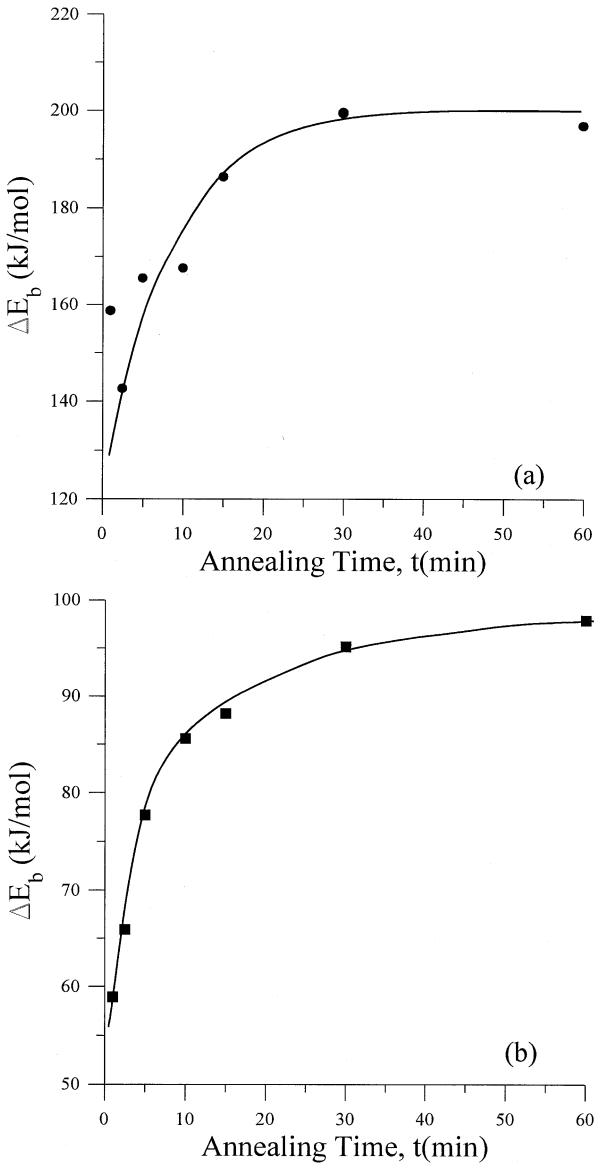

Fig. 10. Plot of backbone activation energies (ΔE_b) versus annealing time (t) for (a) LM, (b) HM films. ΔE_b values are obtained by fitting the stage II data in Figs. 4 and 5 to Eq. (17).

In conclusion, we have shown that simple models for void closure, healing and interdiffusion mechanisms are fitted quite well to our UVV data. Here it has to be noted that all activation energies (ΔH and ΔE_H) are found to be much larger in LM system than HM system. This behaviour can be explained with the annealing temperature range at which the latex systems are treated. Since LM system is annealed at lower temperature range than HM system, polymer chains and segments need higher energies to execute their motion. One has to be realized that ΔH energies of LM and HM system are almost independent of the temperature range of

annealing which emphasize that macroscopic behaviour (viscous flow) of polymeric material is not very sensitive to temperature. However it is observed that the motion of polymer segments (ΔE_H) and backbones (ΔE_b) are very sensitive to the temperature range of annealing.

References

[1] Granier V, Sartre A. Langmuir 1995;11:2179.
[2] Padget JC. J Coatings Technol 1994;66:89.
[3] Müller-Mall R. Macromol Symp 1995;100:159.
[4] Eckersley ST, Rudin A. J Coatings Technol 1990;62(780):89.
[5] Joanicot M, Wong K, Maquet J, Chevalier Y, Pichot C, Graillat C, Linder P, Rios L, Cabane B. Prog Coll Polym Sci 1990;81:175.
[6] Sperry PR, Snyder BS, O'Dowd ML, Lesko PM. Langmuir 1994;10:2619.
[7] Mackenzie JK, Shuttleworth R. Proc Phys Soc 1949;62:838.
[8] Voyutskii SS. Autohesion and adhesion of high polymers. New York: Wiley-Interscience, 1963.
[9] de Gennes PG. J Chem Phys 1971;55:572.
[10] Prager S, Tirrell M. J Chem Phys 1981;75:5194.
[11] Wool RP, O'Connor KM. J Appl Phys 1981;52:5953.
[12] Vanderhoff JW. Br Polym J 1970;2:161.
[13] Distler D, Kanig G. Colloid Polym Sci 1978;256:1052.
[14] Hahn K, Ley G, Schuller H, Oberthur R. Colloid Polym Sci 1988;66:631.
[15] Winnik MA, Wang Y, Haley F. J Coatings Technol 1992;64:51.
[16] Pekcan Ö, Winnik MA, Croucher MD. Macromolecules 1990;23:2673.
[17] Canpolat M, Pekcan Ö. J Polym Sci Polym, Phy Ed 1996;34:691.
[18] Canpolat M, Pekcan Ö. Polymer 1995;36:4433.
[19] Pekcan Ö, Canpolat M. J Appl Polym Sci 1996;59:277.
[20] Canpolat M, Pekcan Ö. Polymer 1995;36:2025.
[21] Pekcan Ö. Trends Polym Sci 1994;2:236.
[22] Pekcan Ö, Arda E, Kesenci K, Pişkin E. J Appl Polym Sci 1998;68:1257.
[23] Pekcan Ö, Kemeroğlu F, Arda E. Eur Polym J 1998;34(9):1371.
[24] Pekcan Ö, Arda E. Polym Int 1998;47:231.
[25] Pekcan Ö, Arda E. J Appl Polym Sci 1998;70:339.
[26] Pekcan Ö, Canpolat M, Arda E. Polym Int 1998;47:451.
[27] Pekcan Ö, Arda E. Colloids Surf A 1999;153:537.
[28] Arda E, Bulmuş V, Pişkin E, Pekcan Ö. J Coll Int Sci 1999;213:160.
[29] Pekcan Ö, Winnik MA, Egan L. Macromolecules 1983;16:702.
[30] Keddie JL, Meredith P, Jones RAL, Donald AM. In: Provder T, Winnik MA, Urban MW, editors. Film formation in waterborne coatings, Proceedings of ACS Symposium Series 648. Washington, DC: American Chemical Society, 1996. p. 332–48.
[31] Mc Kenna GB. In: Booth C, Price C, editors. Comprehensive polymer science, vol. 2. Oxford: Pergamon Press, 1989.
[32] Tager A. Physical chemistry of polymers. Moscow: MIR, 1978.
[33] Kim YH, Wool RP. Macromolecules 1983;16:1115.
[34] Wool RP, Yuan BL, McGarel OJ. Polym Engng Sci 1989;29:1340.